Powering Sensors in IoT System by Using Compact Seven Band PIFA Rectenna

Nermeen A. Eltresy [1,2], Dalia M. Elsheakh [2,3], Esmat A. Abdallah [2], and Hadia M. Elhennawy [1]

[1] Electronics and Communication Engineering Department
Ain Shams University, Cairo, Egypt

[2] Microstrip Department
Electronics Research Institute, Giza, 12622, Egypt
nermeen@eri.sci.eg

[3] Hawaii University at Manoa
Hawaii Center for Advanced Communication, Honolulu, 96922, Honolulu, Hawaii, USA

Abstract ─ A compact seven band coplanar waveguide fed planar inverted F antenna (PIFA) is presented. The proposed antenna is designed to harvest the ambient radio frequency energy at GSM 900, GSM 1800, LTE band 11 and 7, UMTS 2100, Wi-Fi 2.4, LTE and WIMAX 5.2. The antenna is simulated using 3D electromagnetic simulators CST and HFSS. Moreover, the antenna is fabricated and it is used to measure the indoor RF spectrum in Egypt. A simple AC to DC converter unit is designed by using HSMS 2850 Schottky diode to convert the collected RF energy to DC energy. The antenna and the AC to DC converter are integrated to form the RF energy harvesting system. The maximum measured efficiency obtained at 2.4 GHz is about 63.7%.

Index Terms─ Ambient RF waves, Energy Harvesting (EH), Internet of things (IoT), Printed F Antenna (PIFA), rectifier, rectenna, Radio Frequency (RF).

I. INTRODUCTION

Internet of things (IoT) is a system that connects anything at any time through the internet to enable exchanging and collecting data [1]. The IoT system consists of six main items which are identification, sensing, communication, computation, services, and semantics. The identification stage is to mark each object by a unique identifier. Then sensors are used to collect data from the objects after that the collected data is sent to the database or cloud to be analyzed for performing the required user actions. Gas, light, and motion are examples of IoT system sensors. The computation services for IoT are processed using microcontrollers. Microcontrollers are devices that use limited power to perform a simple and specific function. The semantics is the final process and it refers to the ability of extracting the knowledge in a smart manner. Semantics also include properly analyzing data collected in order to make sense of the right decision to provide the required service. So, semantic is considered the brain of the IoT by sending the correct request to the right resource [2]. The IoT sensors nodes and controllers need to be powered by an electrical source. Usually the IoT sensors can be replaced anywhere also they may be buried or fixed in a specific location according to the required IoT application. So that batteries are used to power sensors because it will be extremely complex to power the IoT sensors by wire cables. However, the batteries are not the ideal solution for powering these sensors because after a certain time the batteries need to be replaced. As a result of that using energy harvesting for powering IoT sensors is the solution [3].

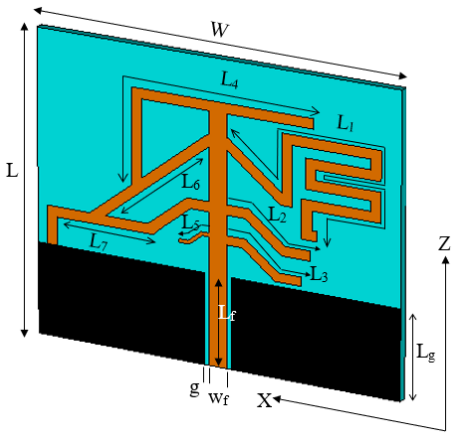

Fig. 1. The structure geometry of optimized antenna.

There are different energy harvesting sources. These

Submitted On: July 5, 2018
Accepted On: November 7, 2018

different sources can be classified into three main categories which are thermal, radiant, and mechanical energy harvesting. The thermal energy can be collected from a body heat or from an external source of heat [4, 5, 6]. The mechanical energy has a lot of shapes like the body motion, vibrations, air flow, and blood flow [7]. The radiant energy can be found in the form of visible light, infrared waves, or radio waves [8].

Nowadays the electromagnetic energy exists in all places (faculties, companies, trading centers, streets). That is because of the spectacular growing of wireless devices and as a result of that the sources of the radiated RF energy have been enlarged. The RF energy is located at the air all the day even at the night but it has distinct levels of power according to the distance from the electromagnetic source. RF energy harvesting system consists of receiving antenna, rectifier, matching circuit in between the antenna and rectifier. So, the overall system is called (rectenna) which means the rectifier integrated to the antenna. There are a lot of antennas which were designed for the ambient RF energy harvesting. In [9] microstrip antenna was used to harvest the ambient power from the downlink GSM-900 system. A novel of dual linear polarization antenna was introduced in [10]. Where the antenna has two ports, the horizontal port was used for the data communication and the vertical port was used for the energy harvesting with a good isolation between the two ports. A CPW broadband fractal antenna was designed for RF energy harvesting in [11] where a simple rectifier circuit was designed at frequency of 2.4 GHz.

The rapid progress of wireless communication makes multiband antennas important. A tri-band microstrip-fed slot antenna was designed for WLAN/ WiMAX applications in [12]. Multi-band (UWB) Multiple Input Multiple Output (MIMO) antenna was designed in [13] to meet the requirement of multi-band/UWB communication applications. In [14] a small-size CPW-feed multi-band planar monopole antenna was introduced. A novel of compact triband coplanar waveguide fed metamaterial antenna was proposed in [15].

In this paper a CPW fed PIFA antenna operates at seven different frequency bands is introduced, Fig. 1. The proposed antenna is designed to harvest RF energy at mobile application frequency bands of GSM 900, LTE band 11 (1.4 GHz), GSM 1800, UMTS 2100, LTE band 7 (2.6 GHz), Wi-Fi 2.4 and WIMAX 5.2 applications. The fundamental operating frequency of proposed antenna is at 0.9 GHz. Its size is reduced by about 36.4% compared to traditional PIFA antenna operating at this frequency. Moreover, the designed antenna has more compact size than the CPW fed PIFA antennas which were designed before at the same frequency 0.9 GHz and at higher frequency 2.4 GHz. The antenna in [16] was designed to operate at 2.5 GHz however it has a large area. While the antennas in [17-19] have compact areas but they have large thickness of 8 mm and they are not compatible with RF energy harvesting.

The paper is organized as the following: Section II presents the proposed antenna design procedure in details. Section III presents the measured results of fabricated antenna and ambient RF spectrum in Egypt. The rectifier design, simulation results, and the measurement results are presented in Section IV. Section V introduces the overall RF system integrated and measured. The conclusion is given in Section VI.

II. ANTENNA DESIGN PROCDEDURE

The antenna is designed on the low-cost FR-4 substrate with a dielectric constant ε_r=4.5, $tan\ \delta$ = 0.02 and substrate thickness equal to 1.6 mm. The antenna has area of $W\times L$. A 50 Ω feeding line with width of W_f and length of L_f is used to feed the antenna. Particle Swarm Optimization (PSO) in the CST program package [20] is used to optimize the antenna reflection coefficient. The separation gap between the feeding line and the ground plane is g. The ground plane length is L_g. By comparing the area between the compact PIFA with dimensions $70\times60\times1.6$ mm^3 and the traditional CPW PIFA with dimensions $110\times60\times1.6$ mm^3 which resonates at the same resonant frequency 900 MHz in Fig. 2 (a), we found that the reduction between the two antennas size is 36.4%. This is indicated in Figs. 2 (a) and 2 (b). In addition to that, the proposed antenna has seven resonant bands. The start point is optimization for (W_f, g) and design of a traditional PIFA fed by CPW in order to operate at 0.9 GHz. The open-ended arm (arm_1) length is shown in Fig. 2 (a) of traditional PIFA antenna is calculated using equation 1 [18]. Where f is the resonant frequency, ε_{eff} is the effective dielectric constant of the substrate:

$$arm_1 = \frac{c}{4f\sqrt{\varepsilon_{eff}}}. \quad (1)$$

A. Antenna design steps

The proposed antenna design steps are as the following: first the short-ended arm of the traditional CPW fed PIFA antenna is sloped by 40° in order to reduce the antenna size as shown in Fig. 2 (a). Second step is performed by meandering the open-ended arm. Meandering of arm_1 reduces the total length from L_a to L_b, as L_a= 91 mm and L_b=63 mm. Then another arm (arm_2) is added as shown in Fig. 2 (b). By adding arm_2 two frequency bands are achieved. After that other three arms of (arm_3, arm_4, arm_5) are added to the antenna, each arm improves the antenna matching and increasing extra band according to the arm length and position. This can be seen in Fig. 3 which indicates the reflection coefficient variation versus frequency for each step in the antenna design. We can notice that by adding extra arm a new resonant frequency appears. Table 1 lists each arm length and the corresponding resonant frequency.

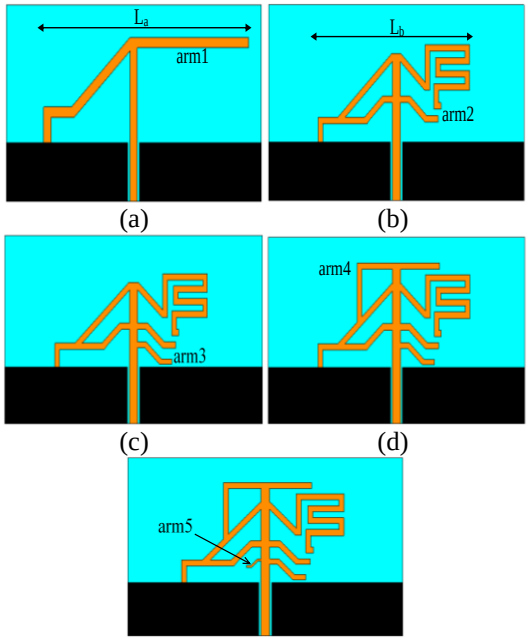

Fig. 2. (a) to (e) Design steps of the proposed antenna.

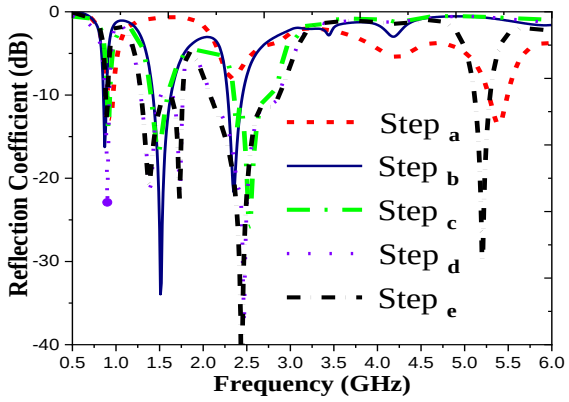

Fig. 3. Reflection coefficient variation versus frequency for design steps of proposed antenna.

Table 1: Antenna arm with corresponding length and frequency

Arm	Length (mm)	Frequency (GHz)
arm_1	47.6	0.9
arm_2	18.3	1.4 and 2.4
arm_3	15	2.6
arm_4	54.2	1.7 and 2.1
arm_5	6.5	5.2

B. Antenna parametric study and optimization

Figures 4 (a), (b) and (c) present reflection coefficient results for the performed study on arm_1, arm_2, and arm_3 lengths, respectively. After each design step, the PSO optimization technique in CST is applied for adjusting PIFA arm's length, width, and position in order to get optimum result at all operating frequency bands. The final optimized antenna is shown in Fig. 1 and the dimensions of the antenna are listed in Table 2. The HFSS is used to verify the final optimized results of CST [20,21]. Figure 6 shows very good agreement between the CST and HFSS results.

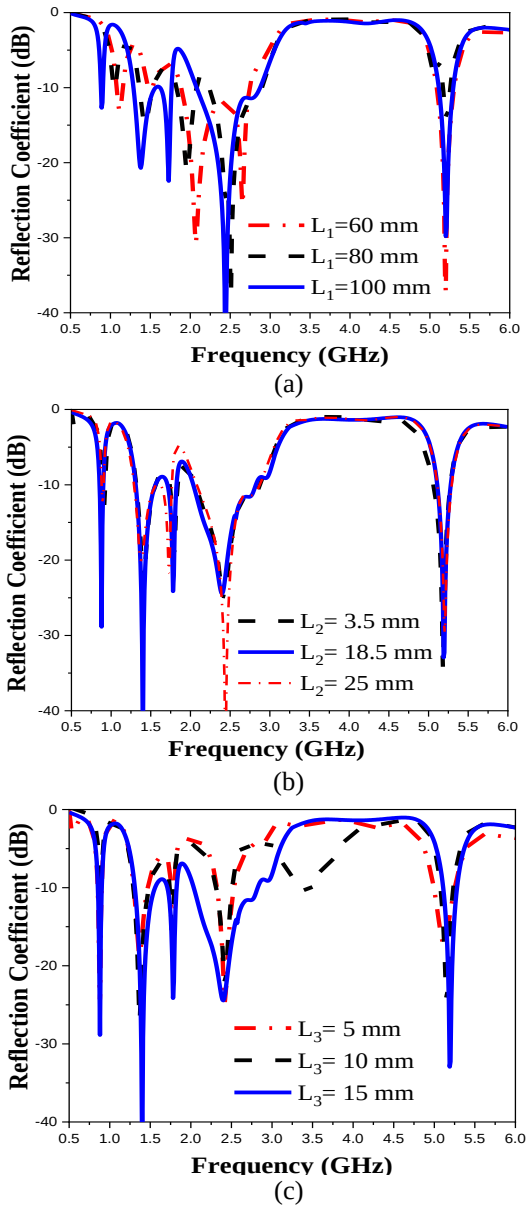

Fig. 4. Reflection coefficient variation versus frequency for different values of: (a) L_1, (b) L_2, and (c) L_3.

The current density distribution on the antenna at different frequencies of 0.9, 1.4, 1.71, 2.1, 2.4, 2.6, and 5.2 GHz is indicated in Fig. 5. The current distribution illustrates that each arm generates a resonant frequency and each arm has a slight effect on the other resonant

frequencies. The simulation values of the antenna gain and radiation efficiency are listed in Table 3.

Table 2: Optimized antenna dimensions (units: *mm*)

L	W	h
70	60	1.6
L_g	L_f	W_f
18	18	3.5
g	L_1	L_2
0.35	100	18.5
L_3	L_4	L_5
15	54.2	6.656
L_6	L_7	
26.4	19	

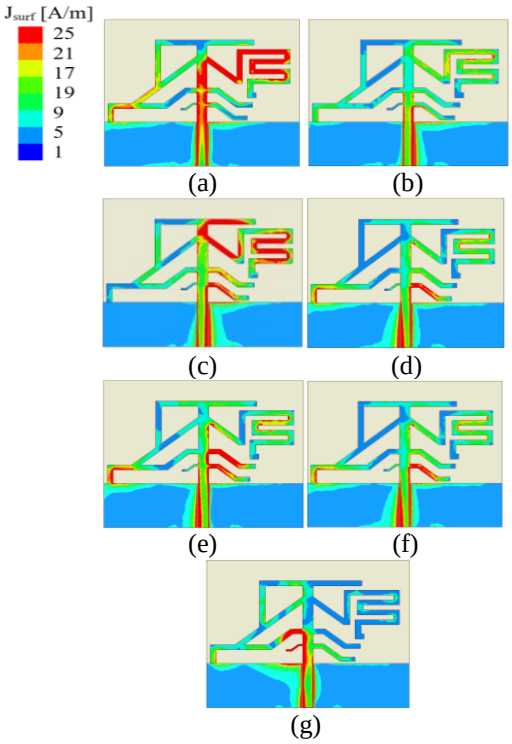

Fig. 5. (a) to (g) Current density distribution of antenna at all antenna frequency resonances at 0.9, 1.4, 1.7, 2.1, 2.4, 2.6, and 5.2GHz, respectively.

Table 3: The simulated radiation characteristics for the proposed antenna

Freq. (GHz)	Gain (dBi)	Rad. Efficiency %
0.9	1.5	90.9
1.4	3	90
1.7	3.4	90.1
2.1	1.1	84.6
2.4	2.12	76.1
2.6	1.1	73
5.2	2.2	60

III. ANTENNA FABRICATION AND RF SPECTRUM MEASUREMENT

The proposed antenna is fabricated. Figure 6 shows the photo of the fabricated antenna and a comparison between the measured and simulated reflection coefficient. There is a good agreement between the simulated and the experimental measured results. The antenna radiation pattern is measured in anechoic chamber with near field system Inc. (NSI) 7005-30 spherical near field system. Comparison between the simulation and the measured radiation patterns of the antenna in E-plane (XZ), and H-plane (XY) at different frequencies are shown in Table 4. Generally, the radiation pattern of the antenna at 0.9, 1.4, 2.6 GHz is omnidirectional in the XZ and XY planes, where at 1.7, 2.4, 5.2 GHz the radiation pattern is directive only in XY plane.

The most difficult thing in the ambient RF energy harvesting system is that ambient power is very low. Unfortunately, the low value of the received power effects on the overall system efficiency. The Friis transmission equation gives the relation between the received power P_r and the transmitted power P_t through a distance R as [9]:

$$p_r = p_t G_t G_r (\frac{\lambda}{4\pi R})^2, \quad (2)$$

where G_t is the transmitting antenna gain, G_r is the receiving antenna gain, and λ is the wavelength of the transmitted signal. The ambient power is measured using the proposed antenna to see the levels of the power at different frequencies. The spectrum measurement was performed using the Agilent Technology N9918A which works as a spectrum analyzer. It can be seen in Fig. 7 the received ambient power variation versus frequency which indicates that there are seven peaks of power. That is because the proposed antenna is a multiband antenna. The maximum values of these peaks and each peak frequency are listed in Table 5.

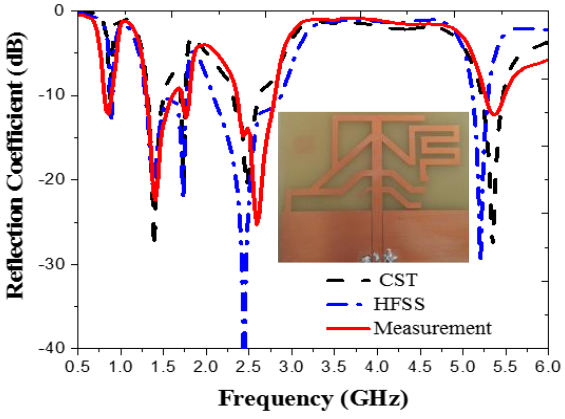

Fig. 6. Photo of the fabricated antenna and comparison between simulated and measured reflection coefficient.

Table 4: The simulated and measured radiation pattern of the CPIFA antenna in the XZ, XY planes at the different operating frequencies. 0.9 GHz, 1.4 GHz, 1.7 GHz, 2.1 GHz, 2.4 GHz, 2.6 GHz, and 5.2 GHz.

Simulation ——— Measurement — · —

Freq.	XZ Plane	XY Plane
0.9 GHz	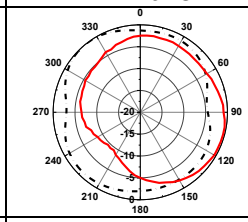	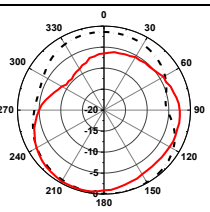
1.4 GHz	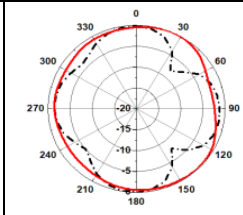	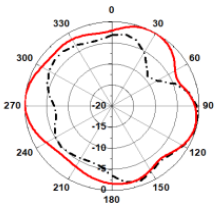
1.7 GHz	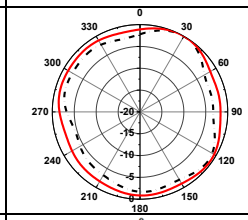	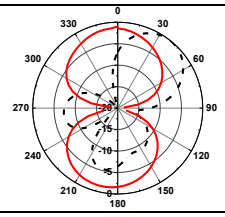
2.1 GHz	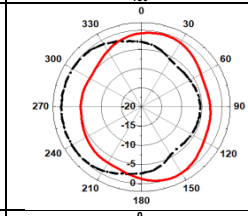	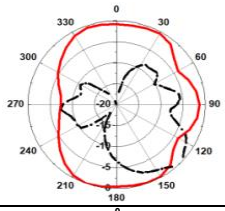
2.4 GHz	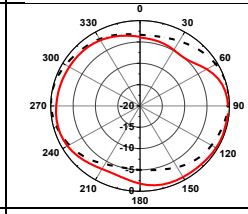	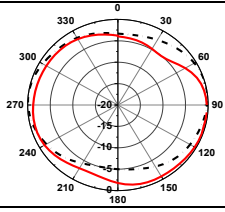
2.6 GHz	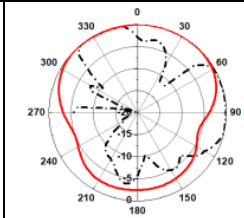	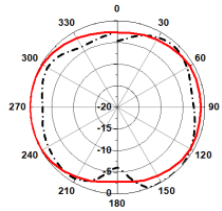
5.2 GHz	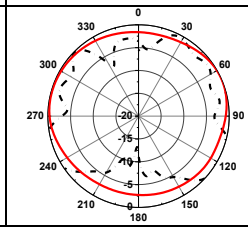	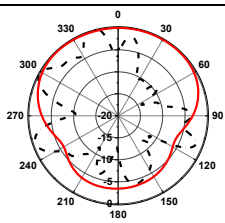

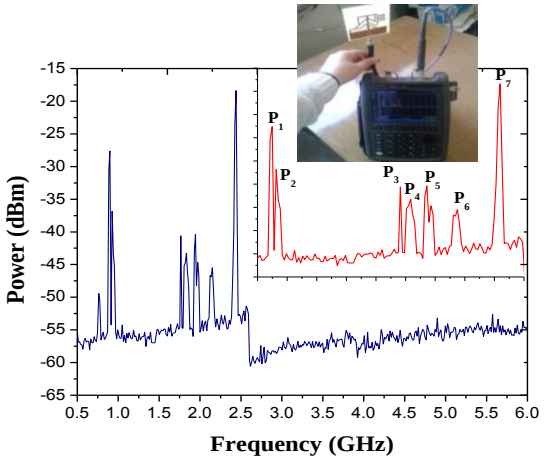

Fig. 7. The received ambient power variation versus frequency using the CPIFA antenna, indoor measurement at 12 pm with photo taken during the spectrum measurement.

Table 5: Values of peaks for recived ambient power using CPIFA antenna

Peak	*Frequency*	*Power* (dBm)	*Power* (μw)
P_1	0.89 GHz	-27.6 dBm	1.7378
P_2	0.92 GHz	-36.8 dBm	0.2089
P_3	1.71 GHz	-40.6 dBm	0.0870
P_4	1.83 GHz	-43.2 dBm	0.0478
P_5	1.94 GHz	-40.3 dBm	0.0933
P_6	2.1 GHz	-45.5 dBm	0.0281
P_7	2.4 GHz	-18.38 dBm	14.5211

IV. RECTIFIER AND MATCHING CIRCUIT

The voltage doubler circuit is designed for converting the received RF power into DC volt and doubling the received voltage. The circuit is designed using HSMS 2850 Schottky diode which has high sensitivity reaches to 150 mV [22] and the output DC volt is taken through output resistance R_L. The equivalent circuit of the diodes is given in Fig. 8 (a). The turn-on voltage of the diode is 150 mV, the breakdown voltage is 3.8V. The resistance R_j is variable with the operating conditions. Using the ADS (Advanced Design System) program, the input impedance of the voltage doubler circuit is found to be 7.9-j105.4, the reflection coefficient is -0.5 dB at 0 dBm input power and 700 Ohm load resistance at 2.4 GHz operating frequency. The impedance of the input source is 50 Ohm. These parameters are used to design the matching circuit with short ended stub between the antenna. Figure 8 (b) shows the rectifier schematic circuit integrated with matching circuit. Different matching circuits are designed at different frequencies. The reflection coefficient variation versus frequency for the three different AC to DC converter unit, where each

one is designed to operate at a specific frequency which are F_1=1.71 GHz, F_2=1.94 GHz, and F_3=2.4 GHz is shown in Fig. 9 (a), Fig. 9 (b) shows comparison between the ADS simulated and measured results of the reflection coefficient when the rectifier attached to the short-ended matching stub of 2.4 GHz.

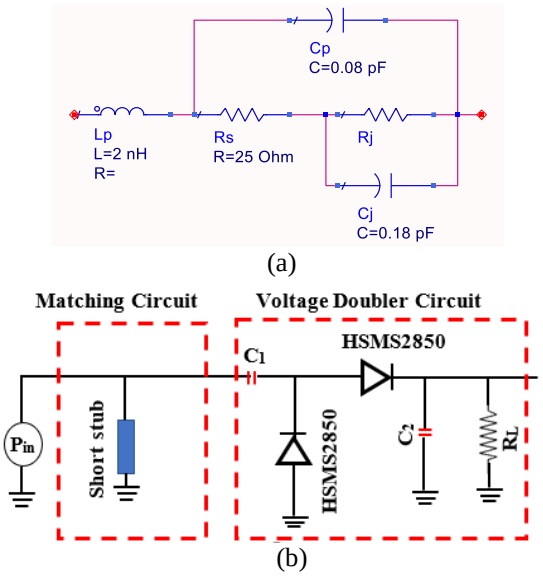

Fig. 8. (a) HSMS2850 equivalent circuit, and (b) single stage voltage doubler.

V. SYSTEM INTEGRATION AND RESULTS

The antenna is integrated with the matching circuit and the voltage doubler circuit. Figure10 (a) shows photo of proposed antenna connected to rectifier circuit. The measurement setup shown in Fig. 10 (b) is used for testing the rectenna system. The Anritsu MG3697C RF is used as a signal generator to feed a wide band horn antenna. Two antennas are used because one of them is connected to spectrum analyzer for recording received value of RF power and the other antenna is integrated with matching circuit and voltage doubler in order to get harvested DC voltage through a parallel connected Tektronix MD04104C oscilloscope for checking DC output wave form versus time variation. Different levels of power are used to feed the horn antenna. Each time the received RF power by proposed antenna is recorded and each corresponding output DC volt is recorded in order to calculate the measurement overall rectenna efficiency.

The rectenna efficiency η is calculated using equations (3) and (4) [10]. The DC output power is $p_{out(DC)}$, the RF input power is $p_{in(RF)}$, $V_{o(DC)}$ is the DC output volt, and the R_L is the load resistance:

$$\eta = \frac{p_{out(DC)}}{p_{in(RF)}}, \tag{3}$$

$$\eta = \frac{V_{o(DC)}^2}{p_{in(RF)} \times R_L}. \tag{4}$$

Comparison between simulated, measured output volt and conversion efficiency variation versus RF input power for rectifier at different frequencies of F_1=1.71 GHz, F_2=1.94 GHz, F_3=2.4 GHz and R_L=700 Ω is shown in Fig. 11 (a) and Fig. 11 (b), respectively.

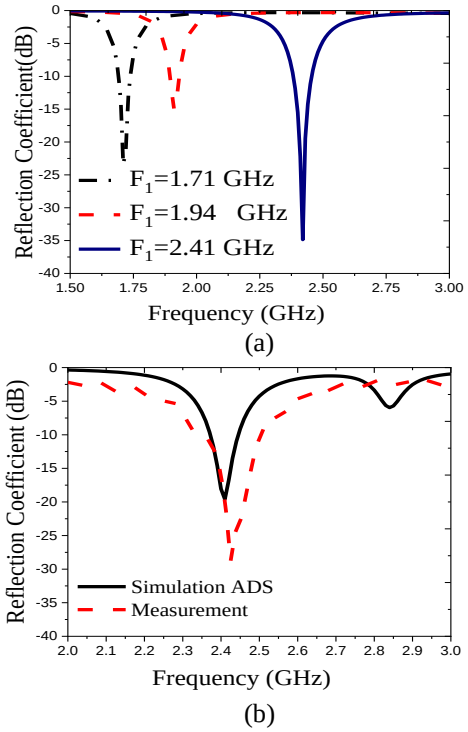

Fig. 9. (a) Reflection coefficient variation versus frequency for three different AC to DC converter unit, and (b) ADS simulated and measured results for rectifier.

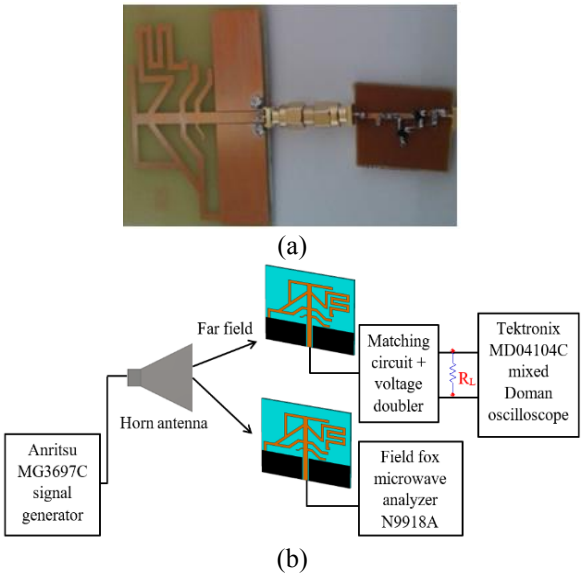

Fig. 10. (a) Photo of rectenna system, and (b) experimental setup for measuring rectenna.

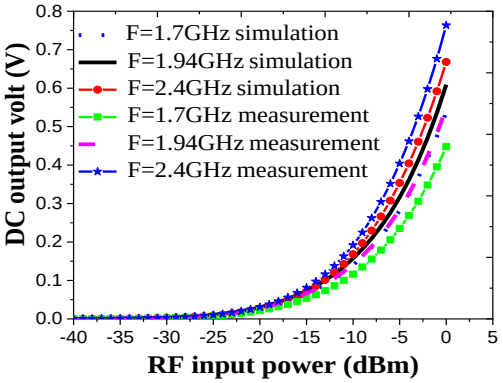

(a)

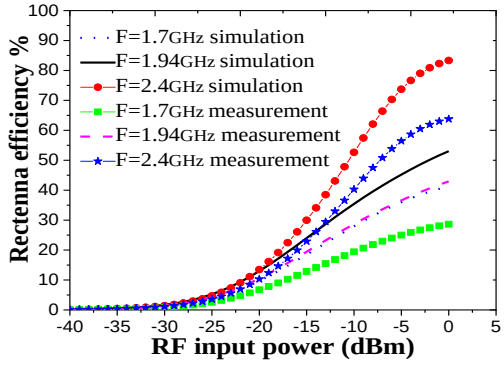

(b)

Fig. 11. Comparison between simulation, measured at R_L=700Ω: (a) DC output volt, and (b) rectenna conversion efficiency versus p_{in}.

Photos for the measured output volt of proposed rectenna using digital multimeter are shown in Figs. 12 (a) and (b), where the output DC volt is 61.4 mV, 129.6 mV at RF received power of -15 dBm, -10 dBm, respectively at 1.94 GHz, and R_L=700Ω. Table 6 lists the values of measured V_o (mV) and η% at different RF input power. The comparison between other rectennas reported previously and our proposed rectenna is listed in Table 7. It can be seen that our design has advantage of high conversion efficiency in low input power level.

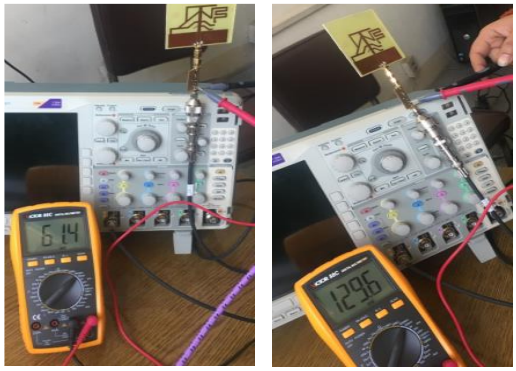

(a) P_{in} =-15 dBm (b) P_{in} =-10 dBm

Fig. 12. The measured output volt of the proposed rectenna using digital multimeter at F_2=1.94 GHz and R_L=700 Ω.

Table 6: Values of measured V_o (mV) and η%

	pin=-15dBm		***Pin=-10dBm***		***Pin=-5dBm***	
Freq	V_o	η%	V_o	η%	V_o	η%
F_1	53	12.6	116	19.2	235	24.9
F_2	61	16.8	130	24.1	284	36.4
F_3	80	28.9	190	51.5	353.5	56.3

Table 7: Comparison between rectennas reported previsouly and the proposed rectenna

Ref.	Frequency (GHz)	Antenna Size (mm^3)	Maximum Gain (dBi)	Input Power Level (dBm)	Conversion Efficiency %
[11]	0.88-8.45	100×100×1.6	8.7	0	51.8
[23]	0.9	62×62×0.254	9	3	48
[24]	0.915 and 2.45	60×60×60	1.87 and 4.18	-9	37 and 30
Proposed rectenna	2.4	79×60×1.6	3.4	-5	56.3

VI. CONCLUSION

Compact CPW fed PIFA antenna with seven different resonant bands namely GSM 900, LTE 11 (1.4 GHz), GSM 1800, UMTS 2100, WIFI 2.4, LTE 7 (2.6 GHz), and WIMAX 5.2 with 36.4% size reduction was designed and measured. The proposed antenna was used to harvest RF energy for IoT system. The antenna dimensions were optimized. The antenna was fabricated and measured with a good agreement between the simulation results and measurement results. A simple AC to DC converter was designed to convert the RF received power into DC power.

ACKNOWLEDGMENT

This work was funded by the National Telecommunication Regularity Authority (NTRA), Ministry of Communication and Information Technology, Egypt. We would like to express our sincere gratitude to Professor Ahmed Attiya because of his help and support for the measurement results.

REFERENCES

[1] L. Atzoria, A. Ierab, and G. Morabito, "The internet of things: A survey," *Computer Networks*, vol. 54, no. 15, pp. 2787-2805, Oct. 2010.

[2] R. Arpita, K. Saxena, and A. A. Bhadra, "Internet of things," *International Journal of Engineering Studies and Technical Approach*, vol. 1, no. 4, pp. 36-42, Apr. 2015.

[3] C. Knight, J. Davidson, and S. Behrens, "Energy options for wireless sensor nodes," *Wireless Sensor Technologies and Applications*, vol. 8, no. 12, pp. 8037-8066, Dec. 2008.

[4] H. Wong and Z. Dahari, "Human body parts heat energy harvesting using thermoelectric module," *Conference on Energy Conversion (CENCON)*, Malaysia, 19-20 Oct. 2015.

[5] M. Ashraf and N. Masoumi, "Thermal energy harvesting power supply with an internal startup circuit for pacemakers," *IEEE Transactions on Very Large Scale Integration (VLSI) Systems*, vol. 24, no. 1, pp. 26-37, Jan. 2016.

[6] S. E. Jo, M. K. Kim, M. S. Kim, and Y. J. Kim, "Flexible thermoelectric generator for human body heat energy harvesting," *Electronics Letters*, vol. 48, no. 16, pp. 1013-1015, Aug. 2012.

[7] S. T. Yusuf, A. M. Yatim, A. S. Samosir, and M. Abdulkadir, "Mechanical energy harvesting devices for low frequency applications: revisited," *ARPN Journal of Engineering and Applied Sciences*, vol. 8, no. 7, pp. 504-512, July 2013.

[8] Available:https://www.researchgate.net/profile/Sanjib_Panda2/publication/264889802/figure/fig6/AS:392161456607247@1470509985797/Fig-8-Types-of-ambient-energy-sources-suitable-for-energy-harvesting-Some-energy.jpg

[9] N. M. Din, C. K. Chakrabarty, A. B. Ismail, K. K. A. Devi, and W.-Y. Chen, "Design of RF energy harvesting system for energizing low power devices," *Progress In Electromagnetics Research (PIER)*, vol. 132, pp. 49-69, 2012.

[10] X. Yang, C. Jiang, A. Z. Elsherbeni, F. Yang, and Y.-Q. Wang, "A novel compact printed rectenna for data communication systems," *IEEE Transactions on Antennas and Propagation*, vol. 61, no. 5, pp. 2532-2539, May 2013.

[11] X. Bai, J. Zhang, L. J. Xu, and B. Zhao, "A broadband CPW fractal antenna for RF energy harvesting," *ACES Journal*, vol. 33, no. 5, pp. 482-487, May 2018.

[12] D.-L. Jin, T.-T. Bu, J.-S. Hong, J.-F. Wang, and H. Xiong, "A tri-band antenna for wireless applications using slot-type SRR," *ACES Journal*, vol. 29, no. 1, pp. 47-53, Jan. 2014.

[13] Y. Li, W. Li, and W. Yu, "A multi-band/UWB MIMO/diversity antenna with an enhanced isolation using radial stub loaded resonator," *ACES Journal*, vol. 28, no. 1, pp. 8-20, Jan. 2013.

[14] B. Yan, D. Jiang, and J. Chen, "Triple notch UWB antenna controlled by novel common direction pentagon complementary split ring resonators," *ACES Journal*, vol. 29, no. 5, pp. 422-427, May 2014.

[15] K. L. Sheeja, P. K. Sahu, S. K. Behera, and N. Dakhli, "Compact tri-band metamaterial antenna for wireless applications," *ACES Journal*, vol. 27, no. 115, pp. 947-955, Nov. 2012.

[16] A. M. Soliman, D. M. Elsheakh, and E. A. Abdallah, "Quad band CPW-planar IFA with independent frequency control for wireless applications," *Proceedings of the 2012 IEEE International Symposium on Antennas and Propagation*, Chicago, USA, pp. 1-2, July 2012.

[17] D. M. Elsheakh, A. M. Soliman, and E. A. Abdallah, "Low specific absorption rate hexa-band coplanar waveguide-fed planar inverted-F antenna with independent resonant frequency control for wireless communication applications," in *IET Microwaves, Antennas & Propagation*, vol. 8, no. 4, pp. 207-216, Mar. 2014.

[18] C. L. Tsai, S. M. Deng, C.-K. Yeh, and S.-S. Bor, "CPW-fed PIFA with finite ground plane for WLAN dual-band applications," *2006 IEEE Antennas and Propagation Society International Symposium*, Albuquerque, USA, pp. 4269-42729, 14 July 2006.

[19] A. Soliman, D. Elsheakh, E. Abdallah, and H. El-Henawy, "CPW fed planar IFA with applied electromagnetic band-gap ground plane," *2013 IEEE Antennas and Propagation Society International Symposium (APSURSI)*, Orlando, USA, pp. 282-283, July 2013.

[20] CST Microwave Studio, ver. 2012, Computer Simulation Technology, Framingham, MA, 2012.

[21] Ansoft High Frequency Structure Simulator (HFSS) ver. 14, Ansoft Corp., 2014.

[22] Surface Mount Microwave Schottky Detector Diodes, HSMS-2850/2860 Series Agilent (Hewlett-Packard), 1998.

[23] S. Ladan, N. Ghassemi, A. Ghiotto, and K. Wu, "Highly efficient compact rectenna for wireless energy havrvesting application," *IEEE Microwave Magazine*, vol. 14, no. 1, pp. 117-122, Feb. 2013.

[24] K. Niotaki, S. Kim, S. Jeong, A. Collado, A. Georgiadis, and M. M. Tentzeris, "A compact dual-band rectenna using slot-loaded dual band folded dipole antenna," *IEEE Antennas and Wireless Propagation Letters*, vol. 12, pp. 1634-1637, Dec. 2013.

Nermeen A. Eltresy received the B.S., and M.S. from Menoufia University, Menoufia, Egypt, in May 2012 and January 2016, respectively. Her Master's thesis was about study and design of nanoantennas element and arrays for different applications. She is currently working toward the Ph.D. degree at Ain Shams University. She is a Assistant Researcher from 2016 until now in the Microstrip Department, Electronics Research Institute. She has published 5 papers in periodical Journals and 6 papers in conferences and a book in the area of nanoantennas design and applications.

Dalia M. Elsheakh received the B.Sc., M.Sc. and Ph.D. degrees from Ain Shams University in 1998, 2005 and 2010, respectively. M.S. thesis was on the design of Microstrip PIFA for mobile handsets. Ph.D. Thesis was in Electromagnetic Band-Gap Structure. From 2010 to 2015, she was Assistant Professor and from 2016 until now she is Associate Prof. in Microstrip Dept., Electronics Research Institute. She was Assistant Researcher at the HCAC, College of Engineering, Hawaii University, USA in 2008 and Assistant Prof. in 2014 and 2018. She has published 50 papers in peer-refereed journals and 45 papers in International Conferences.

Esmat A. Abdallah graduated from the Faculty of Engineering and received the M.Sc. and Ph.D. degrees from Cairo University, Giza, Egypt, in 1968, 1972, and 1975, respectively. She was nominated as Assistant Professor, Associate Professor and Professor in 1975, 1980, and 1985, respectively. She has focused her research on microwave circuit designs, planar antenna systems, and recently on EBG structures, UWB components, and antenna and RFID systems. She has authored and coauthored more than 250 research papers in highly cited international journals and in proceedings of international conferences in her field, such as IEEE Transactions on Antenna and Propagation and IEEE Transactions on Microwave Theory Techniques., etc. She supervised more than 70 Ph.D. and M.Sc. thesis. She has been the President of the Electronics Research Institute in Egypt for more than ten years.

Hadia M. El Hennawy received the B.Sc. and the M.Sc. degrees from Ain Shams University, Cairo, Egypt, in 1972 and 1976, respectively, and the Ph.D. degree from the Technische Universität Braunschweig, Germany, in 1982. In 1982, she returned to Egypt and joined the Electronics and Communications Engineering Department, Ain Shams University, as an Assistant Professor. She was nominated an Associate Professor in 1987 and then a Professor in 1992. In 2004, she was appointed as the Vice-Dean for Graduate Study and Research. In 2005, she was appointed as the Dean of the Faculty of Engineering, Ain Shams University. She has focused her research on microwave circuit design, antennas, microwave communication and recently wireless communication. She has been the Head of the Microwave Research Lab since 1982. She has published more than 100 journal and conference papers and supervised more than 50 Ph.D. and M.Sc. students. She was the Editor-in-Chief of the Faculty of Engineering, Ain Shams University, Scientific Bulletin from August 2004 to August 2005 and is a Member of the Industrial Communication Committee in the National Telecommunication Regulatory Authority (NTRA), Educational Engineering Committee in the Ministry of Higher Education, and Space Technology Committee in the Academy of Scientific Research. She is deeply involved in the Egyptian branch activities.